

Commentary

Scaling from fluxes to organic matter: interpreting ^{13}C isotope ratios of plant material using flux models

The isotope ratios of ecosystem fluxes and pools inform us about ecological connections that are otherwise invisible to the human eye at scales ranging from microbes to landscapes, and from seconds to millennia (Fry, 2006). We use mechanistic models to link observations of isotope ratios to underlying physiological processes. These models allow us to retrieve environmental and physiological signals and to test our current theoretical understanding of ecosystem functions. The most common models to describe ^{13}C and ^{18}O isotope ratios in plants are those of Farquhar and coworkers (reviewed in Cernusak *et al.*, 2013, 2016; Ubierna *et al.*, 2018; Song *et al.*, 2022). These models describe isotope effects occurring in the leaf during the processes of photosynthesis and transpiration. While photosynthesis and transpiration are instantaneous fluxes, applications often deal with downstream pools, such as leaf or tree-ring organic matter, that integrate signals over different timeframes and processes. Scientists have tried to account for this temporal and spatial variation using both simplified (Farquhar & Richards, 1984) and more elaborate (Schiestl-Aalto *et al.*, 2021) models. Nevertheless, 40 years after the initial applications of stable isotopes in ecophysiology, we are still deciphering how environmental signals are recorded by different plant pools. A significant step forward would be understanding the processes that determine the isotope ratios of the leaf sugar pool and how best to model them, as this is ultimately what gets exported to supply dry-matter production. What integration time does the leaf sugar pool $\delta^{13}\text{C}$ and $\delta^{18}\text{O}$ reflect and are there any post-photosynthetic isotope effects already observed within this pool? In this issue of *New Phytologist*, Leppä *et al.* (2022; pp. 2044–2060) addressed this topic by exploring needle sugar C ($\delta^{13}\text{C}$) and O ($\delta^{18}\text{O}$) isotope composition in boreal Scots pine over two growing seasons.

Leppä *et al.* created an environmentally driven dynamic model that predicted $\delta^{13}\text{C}$ and $\delta^{18}\text{O}$ of leaf sugars from leaf-level models of isotope exchange implemented as variants with increasing degrees of complexity. The comparison of model variants found that needle sugar $\delta^{13}\text{C}$ and $\delta^{18}\text{O}$ was reasonably well predicted with relatively simple models, as most of the variation in those signals was related to the c_i/c_a (the ratio of intercellular to ambient $[\text{CO}_2]$) and relative humidity (RH), respectively. These results encourage

the use of tree rings to reconstruct RH and c_i/c_a records. The c_i/c_a values can subsequently be used to estimate intrinsic water-use efficiency (iWUE or A/g_s), a parameter that describes the relationships between water and carbon fluxes, which is used from crop science to global ecology (Farquhar & Richards, 1984; Cernusak, 2020; Saurer & Voelker, 2022).

Nevertheless, 40 years after the initial applications of stable isotopes in ecophysiology, we are still deciphering how environmental signals are recorded by different plant pools.

Applications that retrieve an integrated c_i/c_a from dry matter often use a simplified version of the ^{13}C photosynthetic discrimination model, while a comprehensive model is used to calculate physiological parameters such as mesophyll conductance (g_m). Model simplifications can result in quantitative errors, but comprehensive models can be difficult to parametrize. Choosing an adequate model becomes even more of a challenge when applying the flux models to C pools that have been subjected to metabolism, thereby needing the consideration of post-photosynthetic isotope fractionation. As we struggle to find a balance between model complexity and usefulness, it is important to understand the assumptions and capabilities of each approach. Here, we explain the different models and measurements of C isotope discrimination and how they record and integrate isotope signals. Leppä *et al.* also assess processes across scales that influence the oxygen isotope composition, but we limit this Commentary to ^{13}C processes and refer readers to a recent comprehensive review of ^{18}O effects in leaf water (Cernusak *et al.*, 2016).

Terminology

Discrimination (Δ) indicates the change in isotope ratio between two molecules or compounds induced by a process. That process can be instantaneous (i.e. photosynthesis) or integrative (i.e. synthesis and accumulation of organic compounds). Discrimination can be measured or modelled from theory. We use the following terms: (1) instantaneously observed photosynthetic discrimination against $^{13}\text{CO}_2$ (Δ_{obs} , see Fig. 1 for equations); (2) modelled photosynthetic discrimination ($\Delta_{3\text{-com}}$ or $\Delta_{3\text{-sim}}$); and (3) plant discrimination (Δ_p) measured in organic compounds.

Photosynthetic discrimination (both observed Δ_{obs} and modelled $\Delta_{3\text{-com}}$) describes the change in C isotope composition occurring during photosynthesis, which is a flux with a starting point of ambient CO_2 and an end point of recent assimilates. On the other hand, plant discrimination (Δ_p) determines the change in isotope abundance between ambient CO_2 and organic matter

This article is a Commentary on Leppä *et al.* (2022), 236: 2044–2060.

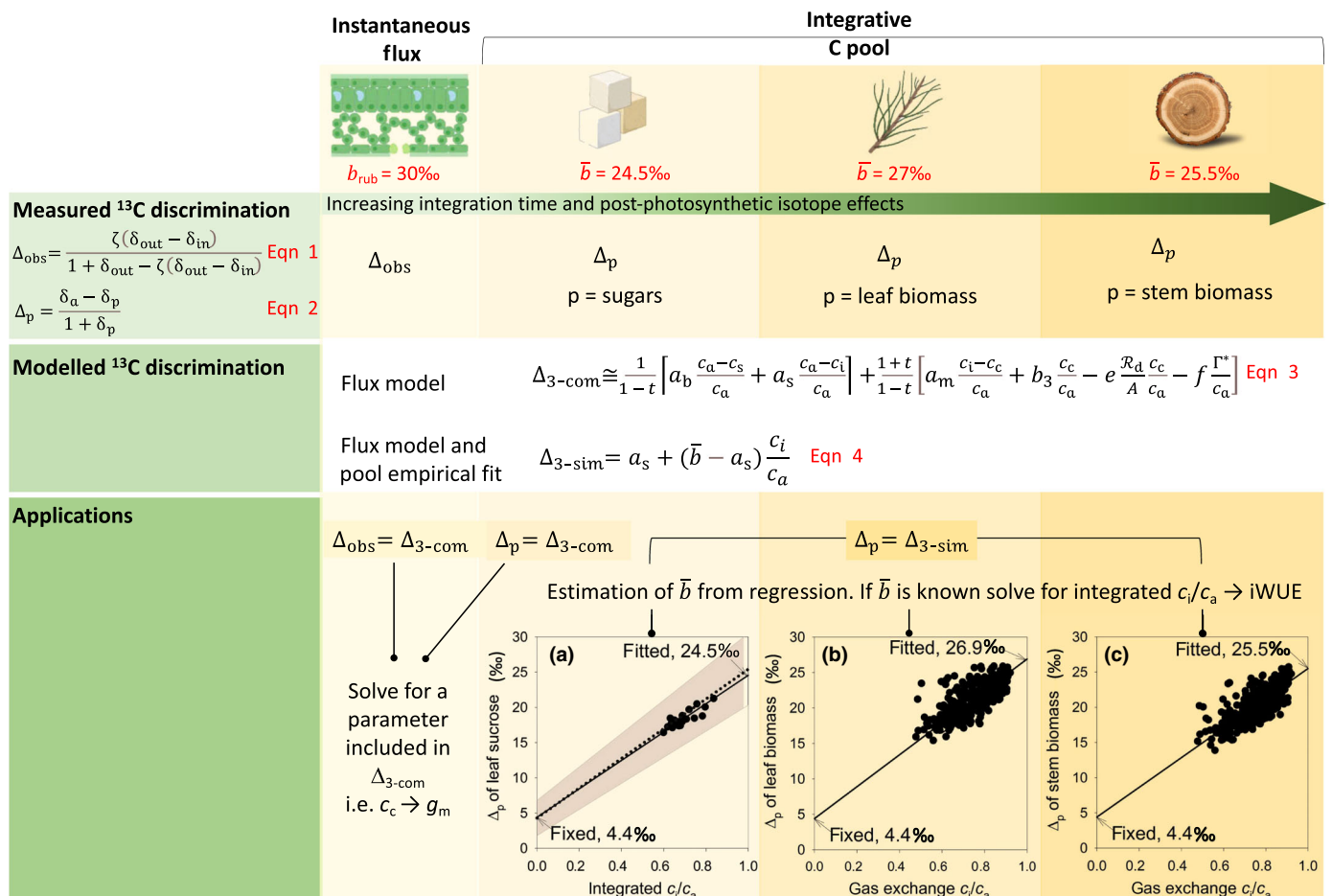


Fig. 1 The C isotope composition ($\delta^{13}\text{C}$) of photosynthate and plant material are partially decoupled; photosynthesis is an instantaneous flux, but plant materials – leaf sugars, leaf biomass and stem biomass – are integrative pools affected by post-photosynthetic processes. The change in C isotope ratio induced during photosynthesis is measured with Δ_{obs} (observed discrimination, Eqn 1, Evans *et al.*, 1986) and modelled with $\Delta_{3\text{-com}}$ (comprehensive model for ^{13}C photosynthetic discrimination, Eqn 3, presented in Busch *et al.*, 2020, format ignoring 'alpha' terms). The change in isotope ratio induced during photosynthesis + post-photosynthetic processes is measured with Δ_{p} (plant discrimination, Eqn 2) but we lack a mechanistic model describing all the processes involved. Instead, a simplified version of $\Delta_{3\text{-com}}$ ($\Delta_{3\text{-sim}}$, Eqn 4) can be used to interpret Δ_{p} values. $\Delta_{3\text{-sim}}$ accounts for post-photosynthetic effects with the parameter \bar{b} , empirically determined from regressions $\Delta_{\text{p}} = a_s + (\bar{b} - a_s)(c_{\text{i}}/c_{\text{a}})$ (solid lines in (a–c), the intercepts are fixed at $a_s = 4.4\text{‰}$ and \bar{b} is fitted and equal to 24.5‰, 26.9‰, and 25.5‰ for sucrose, leaf biomass and stem biomass, respectively). Flux-based applications combine Δ_{obs} and $\Delta_{3\text{-com}}$ to solve for a parameter, such as mesophyll conductance (g_{m}), and allow the investigation of rapid dynamics. Plant biomass applications combine Δ_{p} with $\Delta_{3\text{-sim}}$ to calculate parameters such as intrinsic water-use efficiency (iWUE) over longer periods of time. Δ_{p} derived from sugars pools (i.e. leaves or phloem) has also been combined with $\Delta_{3\text{-com}}$ to derive g_{m} . (a) Closed circles are data from Scots pine needle sucrose in this issue of *New Phytologist* by Leppä *et al.* (2022: pp. 2044–2060) and solid line is the regression fitted to those data points with an intercept of 4.4‰ and slope of 24.5‰; dotted line is $\Delta_{\text{p}} = 4.3 + 21.1(c_{\text{i}}/c_{\text{a}})$, where intercept and slope are the mean values reported in Table 1 and the shaded brown area represents that line ± 1 SD. Data and regression lines in (b, c) are from Cernusák & Ubierna (2022) consisting of 33 woody species (available in 10.5061/dryad.jm63xsjct). Symbols used in equations: $\zeta = c_{\text{in}}/(c_{\text{in}} - c_{\text{out}})$ (unitless), c_{in} , c_{out} , c_{a} , c_{s} , c_{i} and c_{c} are the CO_2 mole fractions ($\mu\text{mol mol}^{-1}$) in the air in and out of a gas-exchange cuvette, ambient air, leaf surface, leaf intercellular spaces and chloroplast, respectively. δ is the $\delta^{13}\text{C}$ (‰) of the incoming (δ_{in}) and outgoing (δ_{out}) air streams, ambient air (δ_{a}) and plant C (δ_{p} , sugars, leaf, stem). a_{b} , a_{s} , a_{m} , e and f are the fractionations associated with diffusion through the boundary layer (2.9‰), in air (4.4‰), in water (1.8‰), during respiration (0‰ to –5‰) and photorespiration (8–16‰), respectively. b_3 is discrimination against ^{13}C by carboxylating enzymes, often taken as rubisco fractionation ($b_{\text{rub}} = 30\text{‰}$). A and R_{d} are the photosynthetic and day respiration rates ($\mu\text{mol m}^{-2} \text{s}^{-1}$), respectively. Γ^* is the CO_2 compensation point in the absence of day respiration ($\mu\text{mol mol}^{-1}$). The ternary effect is $t = \alpha_{\text{ac}}E/2g_{\text{ac}}$, where E is the transpiration rate ($\text{mol m}^{-2} \text{s}^{-1}$), and g_{ac} is the conductance to diffusion of CO_2 in air ($\text{mol m}^{-2} \text{s}^{-1}$).

(e.g. sugars and structural carbohydrates). Recent assimilates and plant matter are partially decoupled in time (instantaneous vs integrative) and space (initial photosynthate vs derived carbohydrates). Accordingly, interpreting $\delta^{13}\text{C}$ signatures of plant matter requires understanding both the turnover time of the pool and the processes downstream of photosynthesis modifying the isotope composition of recent assimilates. The isotope effects

occurring after photosynthesis are referred to as post-photosynthetic fractionations (Badeck *et al.*, 2005). They are numerous, complex to integrate and hinder the physiological interpretation of isotope signals (Gessler & Ferrio, 2022; Kagawa & Battipaglia, 2022). Leppä *et al.* simplified these complexities by assessing leaf sugars (a step closer to assimilates than sugars in sink tissue or the final dry matter).

Despite these complexities, the comparison between measured (Δ_{obs} or Δ_{p}) and modelled ($\Delta_{3\text{-com}}$ or $\Delta_{3\text{-sim}}$) discrimination permits the retrieval of environmental and physiological signals. The comprehensive model for C_3 photosynthetic discrimination ($\Delta_{3\text{-com}}$) includes all the steps in the CO_2 journey during photosynthesis (Farquhar *et al.*, 1982; Farquhar & Cernusak, 2012; Ubierna *et al.*, 2019; Busch *et al.*, 2020). This model can be simplified to a version ($\Delta_{3\text{-sim}}$, Ubierna & Farquhar, 2014) that relates isotope ratios and plant function through a unique variable, the gas exchange parameter c_i/c_a . Neither $\Delta_{3\text{-com}}$ nor $\Delta_{3\text{-sim}}$ explicitly account for post-photosynthetic fractionations as they are flux models. Nevertheless, as discussed subsequently, $\Delta_{3\text{-sim}}$ can indirectly account for post-photosynthetic effects providing a framework to interpret Δ_{p} values.

Using the simplest discrimination model $\Delta_{3\text{-sim}}$

Leaf biomass

The simplest model $\Delta_{3\text{-sim}}$ lumps the combined effects of model simplifications and post-photosynthetic fractionations not considered by the flux model into an empirically determined parameter \bar{b} (Fig. 1). The parameter \bar{b} should not be interpreted as a modified value for b_3 , which is discrimination against ^{13}C by carboxylating enzymes (i.e. mostly rubisco in C_3 plants, but some can also occur by phosphoenolpyruvate). Instead, \bar{b} combines several fractionations that occur during and after photosynthesis. Because post-photosynthetic effects are different across plant tissues, one should not expect a universal \bar{b} value. However, most applications to date have used $\bar{b} = 27\text{‰}$, which was derived from empirical relationships between gas exchange c_i/c_a and Δ_{p} calculated from leaf bulk material (Farquhar *et al.*, 1982; Cernusak *et al.*, 2013; Cernusak & Ubierna, 2022).

Using a parameter derived from leaf biomass to interpret the isotope ratios of other plant tissues has resulted in suboptimal performance of the $\Delta_{3\text{-sim}}$ model, thereby discouraging its use in favor of more complex formulations (Seibt *et al.*, 2008; Gentsch *et al.*, 2014). However, as discussed here, a simplified model $\Delta_{3\text{-sim}}$ can be an acceptable compromise as long as an appropriate \bar{b} is used, which we suggest could have values of c. 27‰, 25.5‰ and 24.5‰ for leaf bulk material, wood and leaf sugars, respectively.

Fractionations occurring during photosynthesis, but neglected in the simplified model, are associated with mesophyll diffusion, respiration and photorespiration. The largest of these, mesophyll diffusion, amounts to a reduction from b_3 to $\bar{b} \cong b_3(c_c/c_i)$ (Ubierna & Farquhar, 2014). The value for rubisco fractionation determined *in vitro* is 30‰ (Roeske & O'Leary, 1984), but it could be lower *in vivo* if some C fixation occurs through phosphoenolpyruvate carboxylation (Farquhar & Richards, 1984; Brugnoli *et al.*, 1988). Using $c_c/c_i = 0.85$ (Ubierna & Farquhar, 2014) and $b_3 = 30\text{‰}$ results in $\bar{b} = 25.5\text{‰}$. Under current ambient conditions (21% O_2 , 400 ppm of CO_2) and at 25°C, photorespiration would further reduce \bar{b} by 1.1‰ (Ubierna & Farquhar, 2014) and respiration is a minor contributor in most situations. Therefore, the combined effects of model simplifications can be balanced out using $\bar{b} \cong 24.5\text{‰}$. This is consistent with the findings of Bickford

et al. (2009), who determined that Δ_{obs} could be approximated with $\Delta_{3\text{-sim}}$ using $\bar{b} = 25\text{‰}$ in *Juniperus monosperma*.

Leaves are 2–3‰ more depleted than nonphotosynthetic tissues (Craig, 1953). Several processes have been suggested to explain this depletion (Cernusak *et al.*, 2009), ranging from variation in biochemical composition (Park & Epstein, 1961; Badeck *et al.*, 2005) to the legacy of depleted structural C added through photosynthesis during leaf expansion, a period when leaves operate at higher c_i/c_a ratios than those typical of mature foliage (Evans, 1983; Vogado *et al.*, 2020). Adjusting the 24.5‰ obtained from model simplifications by the 2–3‰ developmental depletion (larger discrimination with respect to atmospheric CO_2) results in the empirically determined value of $\bar{b} = 27\text{‰}$ for leaf biomass.

Sugar pool

When using a sugar pool, one might expect a value for \bar{b} near 24.5‰ because in this case, the partial decoupling between the measured pool (sugars) and model (instantaneous photosynthate) might only be temporal and will be accounted for by using an integrated c_i/c_a in the model of $\Delta_{3\text{-sim}}$. Nevertheless, there could also exist post-photosynthetic fractionations affecting leaf sugar $\delta^{13}\text{C}$ values. For example, sucrose exported from the leaf has been shown to be more ^{13}C depleted during the day than at night (Gessler *et al.*, 2008). We used Leppä *et al.*'s measured leaf sugar $\delta^{13}\text{C}$ values to produce a relationship Δ_{p} vs weighted c_i/c_a , which had a slope of $20.1 \pm 0.2\text{‰}$ when the intercept was fixed at 4.4‰, and resulted in $\bar{b} = 24.5\text{‰}$ ($\Delta_{\text{p}} = 4.4 + (24.5 - 4.4) c_i/c_a$, $P < 0.0001$, $R^2 = 0.7$, Fig. 1). This \bar{b} is the same as the value we estimated from theory for recent assimilates, suggesting that in Scots pine, the leaf sugar pool was not significantly affected by post-photosynthetic fractionations, but rather it was an integration of the photosynthetic flux (2–5 d).

A value of $\bar{b} = 24.5\text{‰}$ translates to $c_c/c_i \cong 0.82$ (because $\bar{b} \cong b_3(c_c/c_i)$), which is consistent with Leppä *et al.*'s modelling assumption for including g_m in the comprehensive model of ^{13}C discrimination of $c_c/c_i = 0.8$. A similar c_c/c_i ratio has been observed for other C_3 species (Ubierna & Farquhar, 2014). Other approaches have also been used to account for g_m in models of discrimination, such as using a constant g_m (Wingate *et al.*, 2007), a constant ratio of stomata to mesophyll conductance $g_s : g_m$ c. 0.78 (Ma *et al.*, 2021) or equations that calculate g_m from different combinations of parameters such as photosynthetic rate, light, temperature and water stress (Schiestl-Aalto *et al.*, 2021). Here we show that Leppä *et al.*'s data could be predicted with a much simpler model $\Delta_{3\text{-sim}}$ parametrized with $\bar{b} = 24.5\text{‰}$.

To assess the variability associated with \bar{b} , we compiled studies reporting the linear relationship between Δ_{p} from leaf sugars and c_i/c_a (Table 1). These studies used a variety of species (poplar, cotton, bean, sugar beet and rice) and treatments (drought, irradiance, different vegetative states, and age). On average, the slope and intercepts reported in these studies (mean and SD, $n = 8$) were 21.1‰ (2.6) and 4.3‰ (2.5), respectively. A slope of 21.1‰ translates into $\bar{b} = 25.4\text{‰}$ (if a is the average intercept of 4.3‰, Table 1). The 1‰ offset between this mean \bar{b} and the value we calculated with Leppä *et al.*'s data could be related to the fact that

Table 1 Studies reporting $\Delta_p = \text{Intercept} + \text{slope} (c_i/c_a)$ where Δ_p is calculated with Eqn 2 (see Fig. 1) using leaf sugar $\delta^{13}\text{C}$.

Reference	Species	Slope (‰)	Intercept (‰)	Driver of c_i/c_a variation
Brugnoli <i>et al.</i> (1988)	<i>Populus nigra</i> L. × <i>Populus deltoides</i> Marsh <i>Gossypium hirsutum</i> L. <i>Phaseolus vulgaris</i> L.	21.3	3.9	VPD, light intensity and CO ₂
Scartazza <i>et al.</i> (1998)	<i>Oryza sativa</i> L. vegetative state	20.1	6.2	Drought and developmental state
	<i>O. sativa</i> L. flowering	26.6	−0.5	
	<i>O. sativa</i> L. grain filling	22.0	2.1	
Monti <i>et al.</i> (2006)	<i>Beta vulgaris</i> L. 5 DAS	21.3	6.3	Drought and crop ageing
	<i>B. vulgaris</i> L. 38 DAS	19.8	4.9	
	<i>B. vulgaris</i> L. 53 DAS	20.1	5.2	
	<i>B. vulgaris</i> L. 71 DAS	17.7	6.6	
Average (SD)		21.1 (2.6)	4.3 (2.5)	

The simplest model for ^{13}C is $\Delta_{3\text{-sim}} = a_s + (\bar{b} - a_s)(c_i/c_a)$ (Farquhar *et al.*, 1982). VPD, vapor pressure deficit. In the Monti *et al.* (2006) data, DAS stands for days after stress imposition, which was drought. Re-watering occurred at DAS 37.

studies in Table 1 analysed water-soluble sugars (sucrose, glucose, fructose and pinitol) while Leppä *et al.*'s study analysed sucrose. Bulk leaf sugars are ^{13}C depleted compared to sucrose, mostly due to the contribution of ^{13}C depleted pinitol (Rinne *et al.*, 2015). The $\delta^{13}\text{C}$ of pinitol has been shown to be almost invariant during a growing season (Rinne *et al.*, 2015), diluting out the signal of the sugar pool $\delta^{13}\text{C}$ (Leppä *et al.*, 2022). Therefore, applications would benefit from calculating Δ_p from sucrose, or empirically removing the contribution of pinitol.

While variation exists and more studies are needed to quantify the impact of using different sugar fractions, on average, \bar{b} for leaf sugars is likely to be $24.5 \pm 1\text{‰}$ (Fig. 1). If this value for \bar{b} , expected from theory and supported by data from Leppä *et al.* and others (Brugnoli *et al.*, 1988; Scartazza *et al.*, 1998; Monti *et al.*, 2006), is demonstrated to apply to other species and conditions, then it would provide an easy means of deriving integrated c_i/c_a from sugar-derived Δ_p . An integrated c_i/c_a can be preferred over instantaneous gas exchange c_i/c_a to capture plant function, particularly in field settings where collecting sufficient gas exchange records to grasp photosynthetic dynamics is unfeasible. Values of $\delta^{13}\text{C}$ for stem phloem have been demonstrated to integrate the activity of the entire canopy (Ubierna & Marshall, 2011). Therefore, sugar pools can serve to derive integrative physiological parameters that combine with records from eddy flux or remote sensing.

Wood

Tree-ring wood has been found to be 1–2‰ more depleted in ^{13}C than in phloem sugars (Wei *et al.*, 2014) but 1–3‰ enriched compared to leaves (Cernusak *et al.*, 2009). That would suggest a \bar{b} for wood in between those derived for sugars (24.5‰) and leaves (27‰). Indeed this expectation has been confirmed via a regression analysis between Δ_p derived from wood $\delta^{13}\text{C}$ and gas exchange c_i/c_a revealing a value for $\bar{b} = 25.5\text{‰}$ (Cernusak & Ubierna, 2022; Fig. 1). Though much debate still exists regarding post-photosynthetic fractionations, processes such as bark photosynthesis and refixation, or different C storage and remobilization dynamics could explain the ^{13}C offset between wood and sugars (Gessler & Ferrio, 2022).

The value $\bar{b} = 25.5\text{‰}$ was determined with whole wood, but it would need to be readjusted if using cellulose, which is known to be *c.* 1‰ more enriched than wood (Harlow *et al.*, 2006). Values for \bar{b} are empirically derived from a linear regression with the form of the simplest model $\Delta_{3\text{-sim}}$. If one were to use the comprehensive model, or some intermediate version of it, this would lead to an error if \bar{b} were not adequately readjusted (Bloomfield *et al.*, 2019). An example of an intermediate version is presented in Ubierna & Farquhar (2014) that adds the contribution of photorespiration to the simplest ^{13}C discrimination model, which could be useful when large gradients in temperature, O₂ or CO₂ are expected. Photorespiratory contribution to total discrimination in recent assimilates is *c.* 1.1‰, but we ignore how much of that translates into wood biomass $\delta^{13}\text{C}$.

When is $\Delta_{3\text{-sim}}$ not enough?

Using $\Delta_{3\text{-sim}}$ can be an acceptable compromise for many applications, but it will not suffice when the processes investigated are dynamic enough – across time or species – that they cannot be accounted for with a unique and constant \bar{b} value. That is typically the case of applications measuring instantaneous observed discrimination (Δ_{obs}) to derive physiological parameters. Then, the model of choice should be $\Delta_{3\text{-com}}$ because any model simplification, error or uncertainty will be compounded in the value of the derived parameter. In these situations, even ignoring small effects can have a significant impact; for example, mesophyll conductance was overestimated when ternary effects were ignored (Farquhar & Cernusak, 2012). If the aim is to derive iWUE from Δ_{obs} , mesophyll conductance should be accounted for, but respiratory fractionations, boundary layer conductance and ternary effects are far less influential (Ma *et al.*, 2021). If the focus is interpreting diurnal trends in discrimination, $\Delta_{3\text{-sim}}$ will not be able to explain some processes occurring at low fluxes. For example, a comprehensive model was needed to produce good estimations of iWUE early in the morning (Stangl *et al.*, 2019) or to explain large Δ_{obs} at dawn and dusk (Wingate *et al.*, 2007). Interpreting intra-annual trends in tree rings can require models with more than one substrate pool (Offermann *et al.*, 2011).

As illustrated, there are multiple examples where isotope signals cannot be retrieved with $\Delta_{3\text{-sim}}$. However, for broader scale Δ_{p} -based applications, the simplest $\Delta_{3\text{-sim}}$ model is likely to suffice when an appropriate \bar{b} is used. Besides its simplicity, $\Delta_{3\text{-sim}}$ indirectly accounts for photosynthetic and post-photosynthetic effects through the empirically derived value of \bar{b} providing a useful framework to interpret isotope ratios of plant biomass. We encourage scientists to refrain from using $\bar{b} = 27\%$ across the board and instead use tissue-specific values. The values for \bar{b} for both leaves and wood are cross-species averages and the one for sugars is based on Leppä *et al.*'s Scots pine sucrose data and supported by results from other species (Brugnoli *et al.*, 1988; Scartazza *et al.*, 1998; Monti *et al.*, 2006). Variation in \bar{b} exists across species and environmental conditions (Cernusak & Ubierna, 2022). Future research should investigate variation of \bar{b} and how it relates to the many processes lumped into this parameter.

Acknowledgements

Open access publishing facilitated by Australian National University, as part of the Wiley Australian National University agreement via the Council of Australian University Librarians.

ORCID

Graham D. Farquhar  <https://orcid.org/0000-0002-7065-1971>
Meisha-Marika Holloway-Phillips  <https://orcid.org/0000-0002-8353-3536>
Nerea Ubierna  <https://orcid.org/0000-0002-1730-9253>

Nerea Ubierna^{1*} , **Meisha-Marika Holloway-Phillips²** 
and **Graham D. Farquhar¹** 

¹Research School of Biology, The Australian National University, Canberra, ACT 2601, Australia;

²Department of Environmental Science – Botany, University of Basel, Schönbeinstrasse 6, 4056 Basel, Switzerland
(*Author for correspondence: email nerubierna@gmail.com)

References

- Badeck F-W, Tcherkez G, Nogues S, Piel C, Ghashghaie J. 2005. Post-photosynthetic fractionation of stable carbon isotopes between plant organs – a widespread phenomenon. *Rapid Communications in Mass Spectrometry* 19: 1381–1391.
- Bickford CP, McDowell NG, Erhardt EB, Hanson DT. 2009. High-frequency field measurements of diurnal carbon isotope discrimination and internal conductance in a semi-arid species, *Juniperus monosperma*. *Plant, Cell & Environment* 32: 796–810.
- Bloomfield KJ, Prentice IC, Cernusak LA, Eamus D, Medlyn BE, Rumman R, Wright IJ, Boer MM, Cale P, Cleverly J *et al.* 2019. The validity of optimal leaf traits modelled on environmental conditions. *New Phytologist* 221: 1409–1423.
- Brugnoli E, Hubick KT, von Caemmerer S, Wong SC, Farquhar GD. 1988. Correlation between the carbon isotope discrimination in leaf starch and sugars of C₃ plants and the ratio of intercellular and atmospheric partial pressures of carbon dioxide. *Plant Physiology* 88: 1418–1424.
- Busch FA, Farquhar GD, Stuart-Williams H, Holloway-Phillips M. 2020. Revisiting carbon isotope discrimination in C₃ plants shows respiration rules when photosynthesis is low. *Nature Plants* 6: 245–258.
- Cernusak LA. 2020. Gas exchange and water-use efficiency in plant canopies. *Plant Biology* 22: 52–67.
- Cernusak LA, Barbour MM, Arndt SK, Cheesman AW, English NB, Feild TS, Helliker BR, Holloway-Phillips MM, Holtum JAM, Kahmen A *et al.* 2016. Stable isotopes in leaf water of terrestrial plants. *Plant, Cell & Environment* 39: 1087–1102.
- Cernusak LA, Tcherkez G, Keitel C, Cornwell WK, Santiago LS, Knohl A, Barbour MM, Williams DG, Reich PB, Ellsworth DS *et al.* 2009. Viewpoint: Why are non-photosynthetic tissues generally ¹³C enriched compared with leaves in C₃ plants? Review and synthesis of current hypotheses. *Functional Plant Biology* 36: 199–213.
- Cernusak LA, Ubierna N. 2022. Carbon isotope effects in relation to CO₂ assimilation by tree canopies. In: Siegwolf RTW, Brooks JR, Roden J, Saurer M, eds. *Stable isotopes in tree rings. Tree physiology, vol. 8*. Cham, Switzerland: Springer, 291–310.
- Cernusak LA, Ubierna N, Winter K, Holtum JAM, Marshall JD, Farquhar GD. 2013. Environmental and physiological determinants of carbon isotope discrimination in terrestrial plants. *New Phytologist* 200: 950–965.
- Craig H. 1953. The geochemistry of the stable carbon isotopes. *Geochimica et Cosmochimica Acta* 3: 53–92.
- Evans JR. 1983. *Photosynthesis and nitrogen partitioning in leaves of Triticum aestivum L. and related species*. PhD thesis, Australian National University, Canberra, ACT, Australia.
- Evans JR, Sharkey TD, Berry JA, Farquhar GD. 1986. Carbon isotope discrimination measured concurrently with gas-exchange to investigate CO₂ diffusion in leaves of higher-plants. *Australian Journal of Plant Physiology* 13: 281–292.
- Farquhar GD, Cernusak LA. 2012. Ternary effects on the gas exchange of isotopologues of carbon dioxide. *Plant, Cell & Environment* 35: 1221–1231.
- Farquhar GD, O'Leary MH, Berry JA. 1982. On the relationship between carbon isotope discrimination and the intercellular carbon dioxide concentration in leaves. *Australian Journal of Plant Physiology* 9: 121–137.
- Farquhar GD, Richards RA. 1984. Isotopic composition of plant carbon correlates with water-use efficiency of wheat genotypes. *Australian Journal of Plant Physiology* 11: 539–552.
- Fry B. 2006. *Stable isotope ecology*. New York, NY, USA: Springer-Verlag.
- Gentsch L, Hammerle A, Sturm P, Ogée J, Wingate L, Siegwolf R, Pliiss P, Baur T, Buchmann N, Knohl A. 2014. Carbon isotope discrimination during branch photosynthesis of *Fagus sylvatica*: a Bayesian modelling approach. *Plant, Cell & Environment* 37: 1516–1535.
- Gessler A, Ferrio JP. 2022. Postphotosynthetic fractionation in leaves, phloem and stem. In: Siegwolf RTW, Brooks JR, Roden J, Saurer M, eds. *Stable isotopes in tree rings. Tree physiology, vol. 8*. Cham, Switzerland: Springer, 381–396.
- Gessler A, Tcherkez G, Peuke AD, Ghashghaie J, Farquhar G. 2008. Experimental evidence for diel variations of the carbon isotope composition in leaf, stem and phloem sap organic matter in *Ricinus communis*. *Plant, Cell & Environment* 31: 941–953.
- Harlow BA, Marshall JD, Robinson AP. 2006. A multi-species comparison of $\delta^{13}\text{C}$ from whole wood, extractive-free wood and holocellulose. *Tree Physiology* 26: 767–774.
- Kagawa A, Battipaglia G. 2022. Post-photosynthetic carbon, oxygen and hydrogen isotope signal transfer to tree rings – how timing of cell formations and turnover of stored carbohydrates affect intra-annual isotope variations. In: Siegwolf RTW, Brooks JR, Roden J, Saurer M, eds. *Stable isotopes in tree rings. Tree physiology, vol. 8*. Cham, Switzerland: Springer, 429–462.
- Leppä K, Tang Y, Ogée J, Launiainen S, Kahmen A, Kolari P, Sahlstedt E, Saurer M, Schiestl-Aalto P, Rinne-Garmston KT. 2022. Explicitly accounting for needle sugar pool size crucial for predicting intra-seasonal dynamics of needle carbohydrates $\delta^{18}\text{O}$ and $\delta^{13}\text{C}$. *New Phytologist* 236: 2044–2060.
- Ma WT, Tcherkez G, Wang XM, Schäufele R, Schnyder H, Yang Y, Gong XY. 2021. Accounting for mesophyll conductance substantially improves ¹³C-based estimates of intrinsic water-use efficiency. *New Phytologist* 229: 1326–1338.
- Monti A, Brugnoli E, Scartazza A, Amaducci MT. 2006. The effect of transient and continuous drought on yield, photosynthesis and carbon isotope discrimination in sugar beet (*Beta vulgaris* L.). *Journal of Experimental Botany* 57: 1253–1262.

- Offermann C, Ferrio JP, Holst J, Grote R, Siegwolf R, Kayler Z, Gessler A. 2011. The long way down – are carbon and oxygen isotope signals in the tree ring uncoupled from canopy physiological processes? *Tree Physiology* 10: 1088–1102.
- Park R, Epstein S. 1961. Metabolic fractionation of C¹³ and C¹² in plants. *Plant Physiology* 36: 133–138.
- Rinne KT, Saurer M, Kirilyanov AV, Loader NJ, Bryukhanova MV, Werner RA, Siegwolf RTW. 2015. The relationship between needle sugar carbon isotope ratios and tree rings of larch in Siberia. *Tree Physiology* 35: 1192–1205.
- Roeske CA, O'Leary MH. 1984. Carbon isotope effects on the enzyme-catalyzed carboxylation of ribulose biphosphate. *Biochemistry* 23: 6275–6284.
- Saurer M, Voelker S. 2022. Intrinsic water-use efficiency derived from stable carbon isotopes of tree-rings. In: Siegwolf RTW, Brooks JR, Roden J, Saurer M, eds. *Stable isotopes in tree rings. Tree physiology, vol. 8*. Cham, Switzerland: Springer, 481–498.
- Scartazza A, Lauteri M, Guido MC, Brugnoli E. 1998. Carbon isotope discrimination in leaf and stem sugars, water-use efficiency and mesophyll conductance during different developmental stages in rice subjected to drought. *Australian Journal of Plant Physiology* 25: 489–498.
- Schiestl-Aalto P, Stangl ZR, Tarvainen L, Wallin G, Marshall J, Mäkelä A. 2021. Linking canopy-scale mesophyll conductance and phloem sugar $\delta^{13}\text{C}$ using empirical and modelling approaches. *New Phytologist* 229: 3141–3155.
- Seibt U, Rajabi A, Griffiths H, Berry JA. 2008. Carbon isotopes and water use efficiency: sense and sensitivity. *Oecologia* 155: 441–454.
- Song X, Lorrey A, Barbour MM. 2022. Environmental, physiological and biochemical processes determining the oxygen isotope ratio of tree-ring cellulose. In: Siegwolf RTW, Brooks JR, Roden J, Saurer M, eds. *Stable isotopes in tree rings. Tree physiology, vol. 8*. Cham, Switzerland: Springer, 311–329.
- Stangl ZR, Tarvainen L, Wallin G, Ubierna N, Röntfors M, Marshall JD. 2019. Diurnal variation in mesophyll conductance and its influence on modelled water-use efficiency in a mature boreal *Pinus sylvestris* stand. *Photosynthesis Research* 141: 53–63.
- Ubierna N, Cernusak LA, Holloway-Phillips M, Busch FA, Cousins AB, Farquhar GD. 2019. Critical review: incorporating the arrangement of mitochondria and chloroplasts into models of photosynthesis and carbon isotope discrimination. *Photosynthesis Research* 141: 5–31.
- Ubierna N, Farquhar GD. 2014. Advances in measurements and models of photosynthetic carbon isotope discrimination in C₃ plants. *Plant, Cell & Environment* 37: 1494–1498.
- Ubierna N, Holloway-Phillips MM, Farquhar GD. 2018. Using stable carbon isotopes to study C₃ and C₄ photosynthesis: models and calculations. In: Covshoff S, ed. *Photosynthesis. Methods in molecular biology*. New York, NY, USA: Humana Press, 155–196.
- Ubierna N, Marshall JD. 2011. Estimation of canopy average mesophyll conductance using $\delta^{13}\text{C}$ of phloem contents. *Plant, Cell & Environment* 34: 1521–1535.
- Vogado NO, Winter K, Ubierna N, Farquhar GD, Cernusak LA. 2020. Directional change in leaf dry matter $\delta^{13}\text{C}$ during leaf development is widespread in C₃ plants. *Annals of Botany* 126: 981–990.
- Wei L, Marshall JD, Link TE, Kavanagh KL, Du E, Pangle RE, Gag PJ, Ubierna N. 2014. Constraining 3-PG with a new $\delta^{13}\text{C}$ submodel: a test using the $\delta^{13}\text{C}$ of tree rings. *Plant, Cell & Environment* 37: 82–100.
- Wingate L, Seibt U, Moncrieff JB, Jarvis PG, Lloyd J. 2007. Variations in ¹³C discrimination during CO₂ exchange by *Picea sitchensis* branches in the field. *Plant, Cell & Environment* 30: 600–616.

Key words: ¹³C isotope ratios, ecosystem fluxes, flux models, photosynthesis, photosynthetic discrimination, plant material, sugars, tree rings.